

## Article

# Magnetic Properties of Novel Layered Disulfides $\text{CuCr}_{0.99}\text{Ln}_{0.01}\text{S}_2$ (Ln = La ... Lu)

Evgeniy V. Korotaev , Mikhail M. Syrokvashin, Irina Yu. Filatova and Valentina V. Zvereva

Nikolaev Institute of Inorganic Chemistry, Siberian Branch of Russian Academy of Sciences, 630090 Novosibirsk, Russia; syrokvashin@niic.nsc.ru (M.M.S.); rare@niic.nsc.ru (I.Y.F.); zvereva@niic.nsc.ru (V.V.Z.)

\* Correspondence: korotaev@niic.nsc.ru

**Abstract:** The comprehensive study of the lanthanide-doped solid solutions  $\text{CuCr}_{0.99}\text{Ln}_{0.01}\text{S}_2$  (Ln = La ... Lu) magnetic properties was carried out using static magnetochemistry and differential scanning calorimetry techniques. It was shown that magnetic properties of  $\text{CuCr}_{0.99}\text{Ln}_{0.01}\text{S}_2$  are significantly affected by the magnetic properties of the lanthanide ion. The magnetic susceptibility and the effective magnetic moment were found to deviate from the Curie-Weiss law in the temperature 90 K below and 50 K above the order-disorder transition at 695 K. The observed behavior of the temperature dependence of the effective magnetic moment in the order-disorder transition temperature region was described as a result of copper atoms redistribution over different types of the crystallographic sites.

**Keywords:** layered copper-chromium disulfide; lanthanides; magnetic properties; order-to-disorder transition; DSC



**Citation:** Korotaev, E.V.; Syrokvashin, M.M.; Filatova, I.Y.; Zvereva, V.V. Magnetic Properties of Novel Layered Disulfides  $\text{CuCr}_{0.99}\text{Ln}_{0.01}\text{S}_2$  (Ln = La ... Lu). *Materials* **2021**, *14*, 5101. <https://doi.org/10.3390/ma14175101>

Academic Editors: Chander Prakash

Received: 18 August 2021  
Accepted: 3 September 2021  
Published: 6 September 2021

**Publisher's Note:** MDPI stays neutral with regard to jurisdictional claims in published maps and institutional affiliations.



**Copyright:** © 2021 by the authors. Licensee MDPI, Basel, Switzerland. This article is an open access article distributed under the terms and conditions of the Creative Commons Attribution (CC BY) license (<https://creativecommons.org/licenses/by/4.0/>).

## 1. Introduction

The main trends of modern material science are the improvement of existing and the development of new functional materials. Layered chromium dichalcogenides  $\text{CrX}_2$ -based (X = S, Se, Te) compounds can be considered as promising functional materials. The unstable dichalcogenide  $\text{CrX}_2$ -layers can be stabilized by the intercalation of electropositive metal atoms between the adjacent dichalcogenide layers [1,2]. The functional properties of the layered  $\text{CrX}_2$ -based materials could be modified by the cationic substitution of chromium atoms in the dichalcogenide layers or by simultaneous intercalation of metal atoms of different types between  $\text{CrX}_2$ -layers. For instance, in  $\text{CuCrS}_2$ , the unstable  $\text{CrS}_2$ -layers are stabilized by copper atoms. This results in the layered structure of  $\text{CuCrS}_2$  that is formed by the alternating copper and dichalcogenide layers. The  $\text{CuCrS}_2$ -based solid solutions  $\text{CuCr}_{1-x}\text{M}_x\text{S}_2$  are promising functional materials with thermoelectric, superionic, and magnetic properties [3–10]. Chromium atoms could be substituted with other 3d-metal atoms over a wide concentration range ( $x \leq 0.40$ ) without changes in the crystal structure of the initial matrix [6,11,12]. The cationic substitution of  $\text{CuCrS}_2$ -matrix with heavier 3d- or 4f-metal atoms allows one to decrease the thermal conductivity due to the phonon scattering increase [8,13,14]. The reported thermoelectric properties of  $\text{CuCr}_{1-x}\text{M}_x\text{S}_2$  allow one to consider these compounds for the fabrication of high-performance thermoelectric generators (TEGs) [7,8]. The redistribution of copper atoms over the different sites in  $\text{CuCr}_{1-x}\text{M}_x\text{S}_2$ -structure allows one to consider  $\text{CuCrS}_2$ -based solid solutions as promising materials for solid-state power sources, ion-selective membranes, and chemical sensors [6,15,16]. The magnetic properties of  $\text{CuCrS}_2$ -based solid solutions can be used for the fabrication of spin gates, filters, and magnetic memory devices [5,17].

The magnetic properties of the initial  $\text{CuCrS}_2$ -matrix are related to the ferromagnetic ordering of the magnetic moments of chromium atoms in  $\text{CrS}_2$ -layers and to the antiferromagnetic ordering of the adjacent layers. The antiferromagnetic ordering in  $\text{CuCrS}_2$  could be observed at temperatures below the Neel temperature ( $T_N \approx 40$  K). Above  $T_N$

temperature,  $\text{CuCrS}_2$ -matrix and  $\text{CuCr}_{1-x}\text{M}_x\text{S}_2$  solid solutions become paramagnetic and their magnetic susceptibility follows the Curie-Weiss law [2,8,17–21]. As was mentioned above, the phonon scattering has a significant impact on the thermoelectric properties of the material. The phonon scattering enhancement due to the presence of the atoms bearing magnetic moment improves the thermoelectric properties [22]. The cationic substitution of chromium by atoms with different magnetic moment values should significantly affect the phonon scattering efficiency. The magnetic moment of Ln ions is significantly changed across the lanthanide series. Thus, the magnetic properties of the lanthanide-doped  $\text{CuCr}_{1-x}\text{Ln}_x\text{S}_2$  solid solutions are of special interest. As was previously reported, the optimal doping concentration for  $\text{CuCrS}_2$ -based solid solutions is  $x = 0.01$  [7,8]. An increase of  $x$  causes the Seebeck coefficient suppression due to the metal-insulator transition (MIT). Hence, here we report the study of magnetic properties of the lanthanide-doped  $\text{CuCr}_{0.99}\text{Ln}_{0.01}\text{S}_2$  (Ln = La . . . Lu) solid solutions.

$\text{CuCrS}_2$ -based materials exhibit a high-temperature order-disorder transition (ODT). The ODT affects the transport and thermoelectric properties in the high-temperature region ( $T > 670$  K). As the temperature increases, the mobile metal atoms occupy sites that were unoccupied at room temperature. As a result, the electrical conductivity increases. The redistribution of the mobile metal atoms over crystallographic sites in  $\text{CrS}_2$ -sublattice increases a structural disorder. The structural disorder reduces the lattice thermal conductivity resulting from the phonon scattering. Note that the ODT does not significantly affect the crystallographic structure of  $\text{CuCrS}_2$ -matrix and has a reversible character. The magnetic susceptibility temperature dependence of  $\text{CuCr}_{1-x}\text{M}_x\text{S}_2$  follows the Curie-Weiss law in the temperature region above and below the ODT [2,19]:

$$\chi(T) = \frac{C}{T - \theta} = \frac{N_A \mu_B^2}{3k(T - \theta)} \mu_{\text{eff}}^2 \quad (1)$$

where  $T$  is temperature,  $k$  is the Boltzmann constant,  $N_A$  is the Avogadro number,  $\mu_B$  is the Bohr magneton,  $\mu_{\text{eff}}$  is the effective magnetic moment, and  $\theta$  is Weiss constant:

$$\theta = \frac{2j(j+1)}{3k} \sum z_i J_i \quad (2)$$

where  $j$  is the total angular momentum quantum number,  $z_i$  is the magnetic coordination number,  $J_i$  is the exchange interaction between magnetic centers, and  $i$  is the magnetic center number.

However, it should be noted that reported data do not include a detailed study of the magnetic properties in the ODT temperature region. The typical temperature resolution in the corresponding region exceeds 50 degrees [2,8,19]. Nevertheless, the physical properties of  $\text{CuCrS}_2$ -matrix dramatically change in the immediate vicinity of the ODT (about  $\pm 50$  degrees) [3]. Thus, the detailed study of the magnetic properties of  $\text{CuCr}_{0.99}\text{Ln}_{0.01}\text{S}_2$  in the immediate vicinity of the ODT is of special interest and has not been reported yet.

The synthesis procedure significantly affects the magnetic properties of  $\text{CuCrS}_2$ -matrix. The different experimental works report on the contradictory results concerning the effective magnetic moment ( $\mu_{\text{eff}}$ ) and Weiss constant ( $\theta$ ) of  $\text{CuCrS}_2$ . Thus,  $\mu_{\text{eff}}$  and  $\theta$  lie within the wide range of values 3.8 to 5.5  $\mu_B$  and  $-110$  to  $-150$  K, respectively. Furthermore, in case of the cation substituted solid solutions based on  $\text{CuCrS}_2$ -matrix, the Weiss constant values are spread out even more [4,6,7,18,23]. For instance, some of the  $\text{CuCrS}_2$ -based solid solutions were reported to have positive  $\theta$  values [24]. This fact indicates the presence of a significant ferromagnetic contribution to the magnetic susceptibility value. It should be noted that the corresponding contribution could be due to the presence of specific ferromagnetic impurities [21]. Thus, in this study, the ferromagnetic contribution in the magnetic susceptibility value was taken into account.

Here, we report the study of the ODT and cationic substitution effect on the magnetic properties of lanthanide-doped  $\text{CuCr}_{0.99}\text{Ln}_{0.01}\text{S}_2$  ( $\text{Ln} = \text{La} \dots \text{Lu}$ ) solid solutions using both differential scanning calorimetry (DSC) and static magnetochemistry techniques.

## 2. Experimental

The powder samples studied were synthesized from the initial metal oxides using a previously reported procedure [3,8]. The average grain size was 25  $\mu\text{m}$ . The X-ray powder diffraction (XRD) experiment was carried out using non-monochromatic  $\text{CuK}\alpha$ -radiation on a Shimadzu XRD 7000S diffractometer (Shimadzu Corporation, Kyoto, Japan). The XRD patterns were found quite similar. Figure 1 shows typical XRD patterns of the initial matrix and some solid solutions  $\text{CuCr}_{0.99}\text{Ln}_{0.01}\text{S}_2$ . The XRD patterns of all  $\text{CuCr}_{0.99}\text{Ln}_{0.01}\text{S}_2$  ( $\text{Ln} = \text{La} \dots \text{Lu}$ ) synthesized samples are shown in Supplementary Figure S1. The observed diffraction peaks on the XRD pattern indicate that the synthesized  $\text{CuCrS}_2$  sample has a rhombohedral structure with an  $R3m$  space group. The absence of the additional diffraction peaks allows one to conclude that synthesized samples are single-phase. The position and diffraction peaks intensity are in good agreement with the XRD data of the Inorganic Crystal Structure Database (database code 100594, denoted as “ICSD” in Figure 1) [25]. The calculated unit cell parameters  $a = 3.48(3)$  and  $c = 18.71(6)$   $\text{\AA}$  correlate well with the previously reported and reference data [7,25,26]. The lattice parameters of  $\text{CuCr}_{0.99}\text{Ln}_{0.01}\text{S}_2$  are close to those for  $\text{CuCrS}_2$ -matrix and lies within the range of 3.47–3.48 and 18.67–18.71  $\text{\AA}$  for  $a$  and  $c$ , respectively. However, the unit cell volume slightly decreases due to the lanthanide contraction with an increase of the Ln atomic number (Supplementary Table S1 in Supplementary Materials). Thus, one can conclude that cationic substitution by lanthanides does not significantly affect the initial matrix crystal structure.

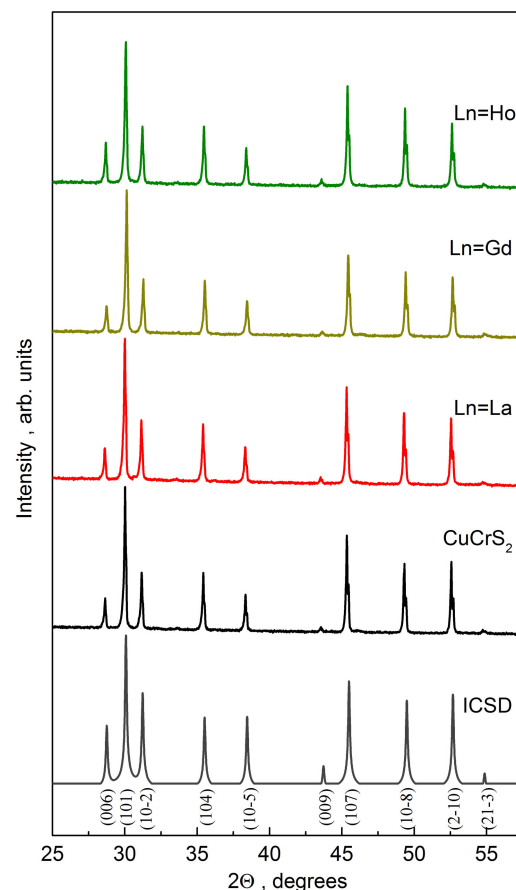


**Figure 1.** Powder diffraction patterns of  $\text{CuCrS}_2$ -matrix and  $\text{CuCr}_{0.99}\text{Ln}_{0.01}\text{S}_2$  solid solutions ( $\text{Ln} = \text{La}, \text{Gd}, \text{Ho}$ ).

The elemental composition of the samples studied was controlled by X-ray fluorescence analysis using a Bruker MISTRAL M1 (Bruker Corporation, Billerica, MA, USA). The composition of the investigated solid solutions correlates well with the reference concentrations (Supplementary Table S2).

The magnetic properties of  $\text{CuCr}_{0.99}\text{Ln}_{0.01}\text{S}_2$  were measured using the Faraday method in the wide temperature range of 80–750 K. The temperature stabilization was controlled using a Delta DTB9696 temperature controller (Delta Electronics, Taipei, Taiwan). The voltage from a quartz torque microbalance was measured using Keysight 34465 A digital voltmeter (Keysight Technologies, Santa-Rosa, CA, USA). The magnetic field strength was varied in the range of 4.8 to 8.6 kOe. The magnetic field strength fluctuations did not exceed 2%. The powder samples (~20 mg) were placed in open quartz ampoules and vacuumed at 0.01 Torr pressure. During the measurements, the samples were held in a helium atmosphere at 5 Torr pressure. The diamagnetic contributions into the magnetic susceptibility value were taken into account using the Pascal scheme. The field dependence of the magnetic susceptibility  $\chi(1/H)$  was measured in order to take into account the possible presence of the ferromagnetic contribution to the magnetic susceptibility value. The effective magnetic moment as a function of temperature was calculated as follows [21,27]:

$$\mu_{\text{eff}}(T) = \sqrt{8\chi T} \quad (3)$$

The thermal effects accompanying the ODT phase transition were studied using a DSC-500 differential scanning calorimeter (LLC Specpribor, Samara, Russia). The powder samples (~15 mg) were placed in open aluminum crucibles. The DSC signals were measured in the argon flow (50 mL/min) at a constant heating rate of 10 °C/min.

### 3. Results and Discussion

Magnetic susceptibility ( $\chi$ ) of chemical compounds is the sum of the different magnetic contributions (paramagnetic, ferromagnetic, and diamagnetic). The diamagnetic contributions are caused by the circulation of the electrons induced by an external magnetic field. The paramagnetic contribution is due to the presence of the unpaired electrons in the material and the field-induced electronic transitions (Van Vleck paramagnetism). The ferromagnetic impurities could significantly affect the magnetic susceptibility value (ferromagnetic contributions). These contributions can be taken into account using the magnetic susceptibility values measured at few different magnetic fields ( $H$ ). The positive slope of  $\chi(1/H)$  indicates the ferromagnetic contribution in the measured magnetic susceptibility value. The  $\chi(1/H)$  behavior of the solid solutions studied were found quite similar. The typical  $\chi(1/H)$  dependencies are shown in Figure 2. The zero slope of  $\chi(1/H)$  indicates that the significant ferromagnetic contribution in  $\chi$  is absent. Thus, one can conclude that the samples studied have no ferromagnetic impurities.

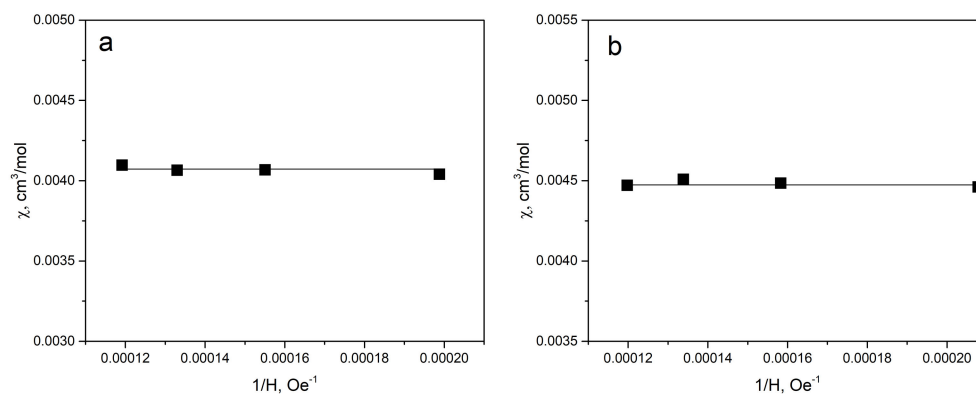


**Figure 2.** Magnetic susceptibility field dependencies  $\chi(1/H)$  at  $T = 300$  K:  $\text{CuCrS}_2$  (a),  $\text{CuCr}_{0.99}\text{Dy}_{0.01}\text{S}_2$  (b).

The behavior of the measured molar magnetic susceptibility temperature dependencies of  $\text{CuCr}_{0.99}\text{Ln}_{0.01}\text{S}_2$  was found quite similar. The typical dependencies of  $\chi(T)$ ,  $1/\chi(T)$ ,  $\mu_{\text{eff}}(T)$  of  $\text{CuCrS}_2$  and several lanthanide-doped solid solutions  $\text{CuCr}_{0.99}\text{Ln}_{0.01}\text{S}_2$  ( $\text{Ln} = \text{La, Nd, Gd, Dy, Er, Lu}$ ) are shown in Figure 3. The Curie-Weiss law (Equation (1)) was used to calculate the effective magnetic moment ( $\mu_{\text{eff}}$ ) and the Weiss constant ( $\theta$ ) values. The  $\mu_{\text{eff}}$  value of  $3.77 \mu_{\text{B}}$  for  $\text{CuCrS}_2$  was in a good agreement with the experimental data reported previously and corresponded to the theoretical value for  $\text{Cr}^{3+}$  state ( $\mu_{\text{eff}}(\text{Cr}^{3+}) = 3.87 \mu_{\text{B}}$ ). Note that for  $\text{CuCrS}_2$  experimental  $\mu_{\text{eff}}$  value, it lay within the range of  $3.75\text{--}3.79 \mu_{\text{B}}$  [5,20,21,26,27]. The Weiss constant of  $-140 \text{ K}$  correlates well with the reported data and lies within the range of  $-110$  to  $-150 \text{ K}$  [5,20,21,23,27].

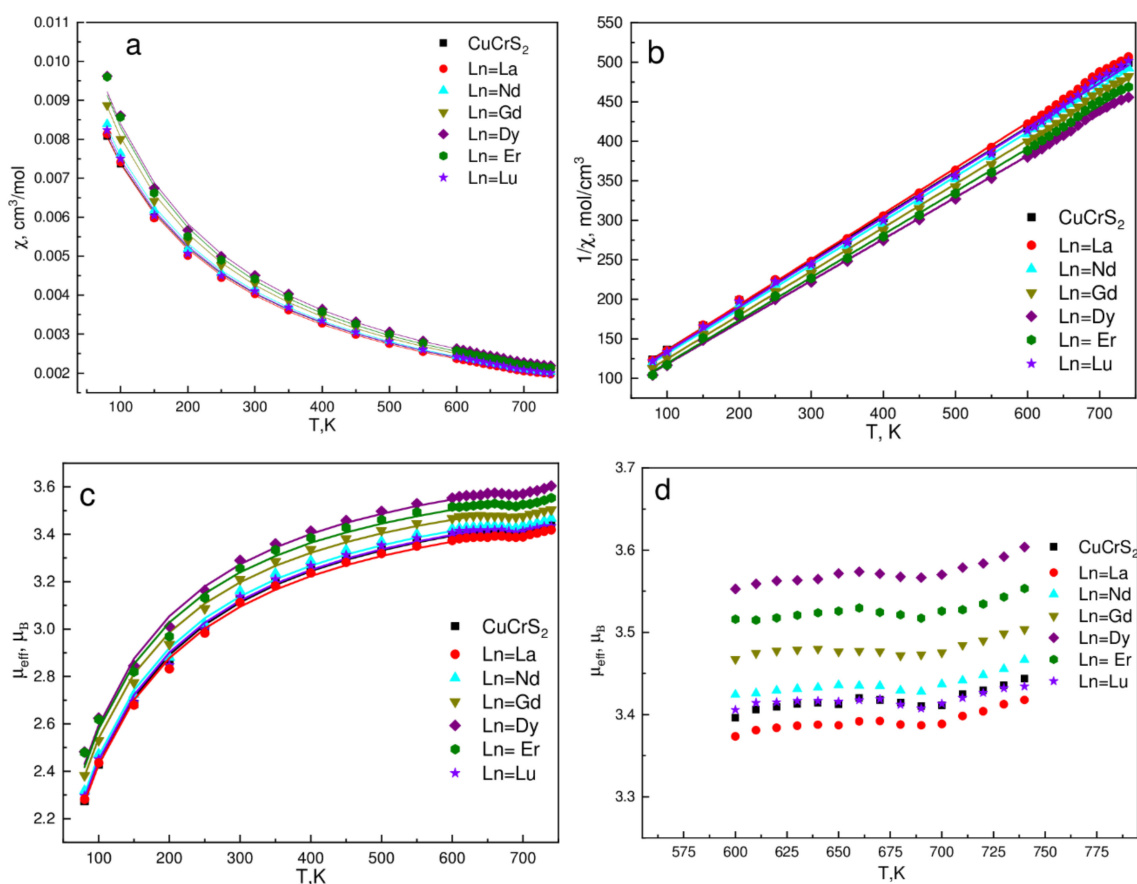


**Figure 3.** Molar magnetic susceptibility (a), inverse magnetic susceptibility (b), and effective magnetic moment (c,d), temperature dependencies. Solid lines are Curie-Weiss law approximation.

The calculated values of  $\mu_{\text{eff}}$  and  $\theta$  for the entire series of the samples studied are plotted in Figure 4a,b. The calculated  $\mu_{\text{eff}}(Z)$  and  $\theta(Z)$  have a non-monotonic behavior ( $Z$  is the lanthanide atomic number). The maximal  $\mu_{\text{eff}}$  value was observed for  $\text{CuCr}_{0.99}\text{Dy}_{0.01}\text{S}_2$ , the minimal one for  $\text{CuCr}_{0.99}\text{La}_{0.01}\text{S}_2$ . Note that in the lanthanide series, the dysprosium and lanthanum atoms have the maximal and the minimal theoretical  $\mu_{\text{eff}}$  value of  $10.6$  and  $0.0 \mu_{\text{B}}$ , respectively [27–29]. Thus, one can conclude that observed  $\mu_{\text{eff}}(Z)$  behavior is associated with the lanthanide magnetic moment. Taking into account the isoivalent cationic substitution character in  $\text{CuCr}_{0.99}\text{Ln}_{0.01}\text{S}_2$  ( $\text{Ln} = \text{La, Ce}$ ) solid solutions [8,30], the theoretical  $\mu_{\text{eff}}(Z)$  could be calculated (Figure 4c). The theoretical  $\mu_{\text{eff}}(Z)$  for  $\text{CuCr}_{0.99}\text{Ln}_{0.01}\text{S}_2$  solid solutions were calculated using table  $\mu_{\text{eff}}$  values of  $\text{Ln}^{3+}$  ions and experimental  $\mu_{\text{eff}}$  value of  $\text{CuCrS}_2$ -matrix [27,29]. The obtained experimental  $\mu_{\text{eff}}(Z)$  correlates well with the theoretical data calculated using non-interacting spin approximation (Figure 3a,c).

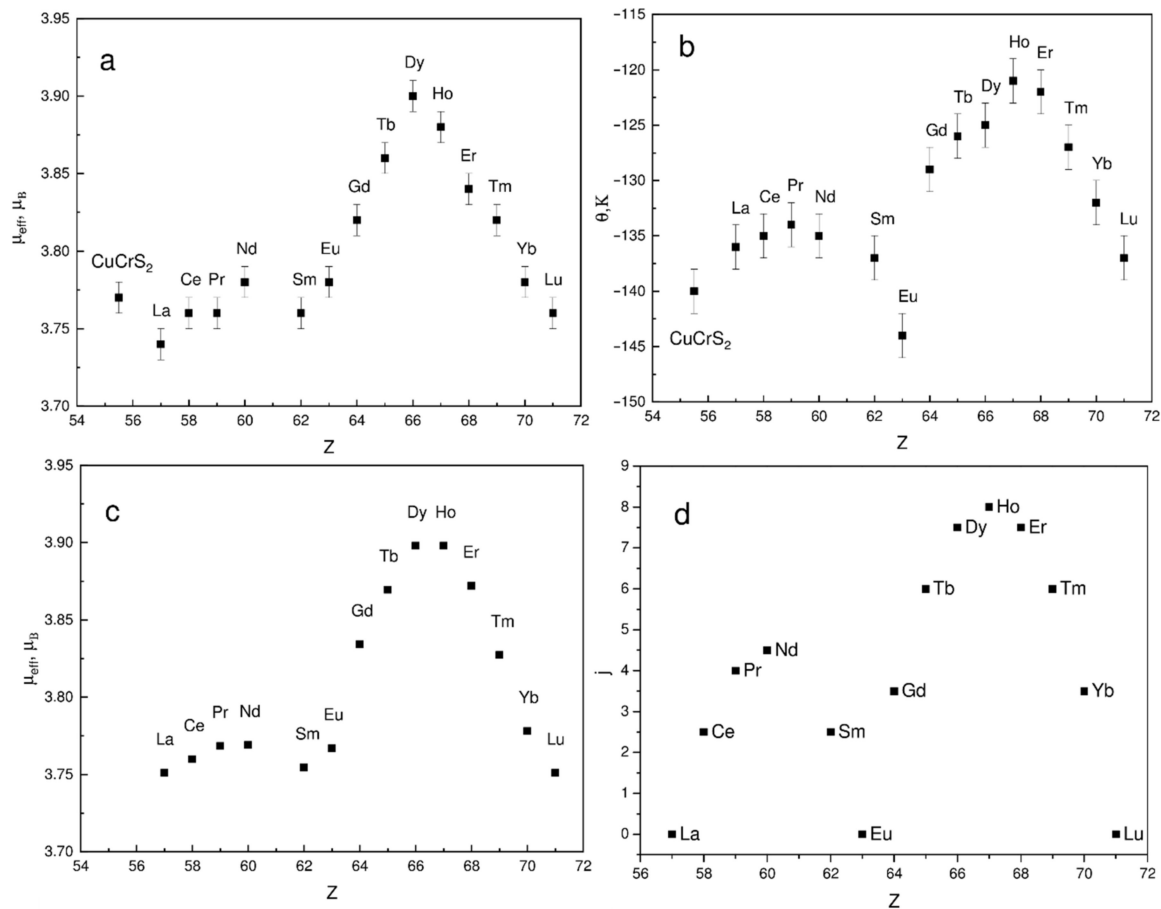


**Figure 4.** Experimental magnetic moment (a), Weiss constant (b), theoretical estimation of  $\mu_{\text{eff}}$  (c), and the total angular momentum quantum number (d) as a function of lanthanide atomic number.

The Weiss constant is related to the exchange interaction between paramagnetic centers. In contrast to CuCrS<sub>2</sub>-matrix, the magnetic properties of CuCr<sub>0.99</sub>Ln<sub>0.01</sub>S<sub>2</sub> are determined not only by the magnetic Cr<sup>3+</sup> ions, but also by Ln<sup>3+</sup> lanthanide ions contributions. Thus, the observed non-linear behavior of  $\theta$  as a function of Z is determined by the lanthanide contribution. In terms of molecular field theory, the Weiss constant is proportional to the spin (for 3d-metals) or to the total angular momentum quantum number  $j$  (for lanthanides). Hence, the theoretical  $j(Z)$  dependence for lanthanide ions was plotted in Figure 4d. Note that both  $j(Z)$  and  $\theta(Z)$  dependencies have a similar behavior (Figure 4b,d). The minimal  $\theta$  values are attributed to the solid solutions doped with lanthanum, europium, and lutetium. This is due to the fact that 4f-orbital is either empty (La) or completely filled (Lu), where  $j = 0$ . The observed Weiss constant decrease for CuCr<sub>0.99</sub>Eu<sub>0.01</sub>S<sub>2</sub> solid solution is due to the spin and orbital magnetic moments compensation (spin-orbit compensation) [31]. Thus, the zero value of  $j$  leads to the absence of the contribution of the lanthanide atoms to the exchange interaction integrals in Equation (2). The decrease of the  $\theta$  absolute value indicates the weakening of the antiferromagnetic interactions after the cationic substitution of chromium with lanthanide atoms with  $j \neq 0$ .

Thus, the behavior of the magnetic properties of the lanthanide-doped solid solutions CuCr<sub>0.99</sub>Ln<sub>0.01</sub>S<sub>2</sub> (Ln = La ... Lu) is majorly determined by the lanthanide ion magnetic properties. Thereby, the most significant effect was observed for lanthanides with the highest  $j$  (from Tb to Er).

As was discussed above, the magnetic properties of CuCr<sub>1-x</sub>Ln<sub>x</sub>S<sub>2</sub> in the ODT temperature region are of special interest. The magnetic susceptibility of the initial copper-chromium disulfide and CuCrS<sub>2</sub>-based solid solutions in the temperature region of 100 to 800 K is commonly described in terms of the Curie-Weiss law [2,6,20]. However, the

improving of the temperature resolution from  $\sim 50$  K to 10 K allows one to observe the deviation from the Curie–Weiss law in the ODT temperature region (Figure 3a). The corresponding effect could be clearly observed in the effective magnetic moment temperature dependencies  $\mu_{\text{eff}}(T)$  (Figure 3c). For clarity, the enlarged curves of  $\mu_{\text{eff}}(T)$  within the temperature range  $\sim 90$  K below and  $\sim 50$  K above the ODT ( $T_{\text{ODT}} \sim 695$  K) are plotted in Figure 3d. The corresponding temperature region exhibits an inflection feature. This fact allows one to conclude that the  $\mu_{\text{eff}}$  value is affected by the ODT. As it was reported previously, the ODT in  $\text{CuCrS}_2$  and similar layered dichalcogenides could be studied using DSC technique [3,13,32]. In this regard, the DSC signals of  $\text{CuCr}_{0.99}\text{Ln}_{0.01}\text{S}_2$  were measured in the same temperature region (Figure 5). The measured DSC signals exhibit a single peak at  $\sim 694$ – $695$  K. Thus, the position of the inflection feature on  $\mu_{\text{eff}}(T)$  dependencies and peak on the DSC curves are correlated well. At room temperature, copper atoms are localized at the “ordered” tetrahedral sites between  $\text{CrS}_2$ -layers, whereas the “disordered” octahedral sites remain unoccupied [10,26,33,34]. With the temperature increase, the occupation probability of octahedral sites increases. Hence, in the temperature region above the ODT, copper atoms are statistically distributed between tetrahedral and octahedral sites. The “ordered” tetrahedral sites were shifted to  $\text{CrS}_2$ -layer, whereas octahedral sites were centered between two adjacent  $\text{CrS}_2$ -layers. Since  $\mu_{\text{eff}}(T)$  decreases at  $T < T_{\text{ODT}}$ , one can conclude that copper atoms in octahedral sites provide more efficient channels for the indirect exchange interaction than atoms in tetrahedral sites. The exchange interaction increase resulted in an increase in the Weiss constant (see Equation (2)). The further temperature increase lead to  $\mu_{\text{eff}}(T)$  an increase at  $T > T_{\text{ODT}}$  due to the magnetic moments disordering of Cr and Ln ions. Thus, the observed  $\mu_{\text{eff}}(T)$  behavior could be associated with the redistribution of the copper atoms over different crystallographic sites caused by the ODT.

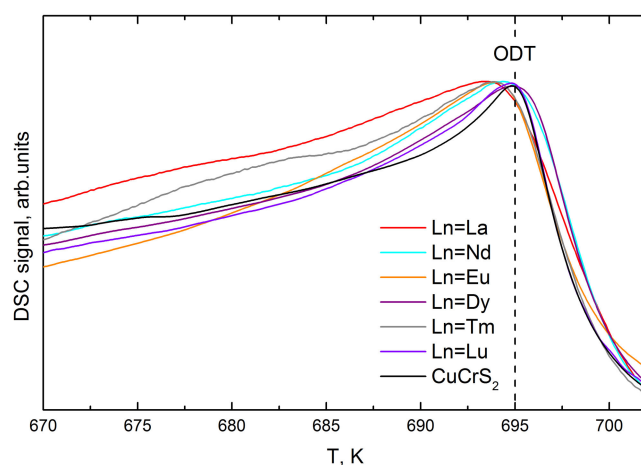


**Figure 5.** DSC-signal of initial  $\text{CuCrS}_2$ -matrix and  $\text{CuCr}_{0.99}\text{Ln}_{0.01}\text{S}_2$  ( $\text{Ln} = \text{La}, \text{Nd}, \text{Eu}, \text{Dy}, \text{Tm}, \text{Lu}$ ) solid solutions in the temperature region of the ODT.

#### 4. Conclusions

A comprehensive study of  $\text{CuCr}_{0.99}\text{Ln}_{0.01}\text{S}_2$  ( $\text{Ln} = \text{La} \dots \text{Lu}$ ) magnetic properties in a wide temperature range of 80–740 K was carried out. It was established that the effective magnetic moment and the Weiss constant of the lanthanide-doped solid solutions are significantly affected by the total angular momentum quantum number  $j$  and the effective magnetic moment of the lanthanide ion. The most significant effect on the magnetic properties was observed for solid solutions doped with Tb, Dy, Ho, and Er. Thus, these lanthanides are the most promising candidates for the modification of  $\text{CuCrS}_2$ -based solid solutions magnetic properties. The magnetic properties’ behavior in the immediate vicinity of the ODT was reported for the first time. The magnetic susceptibility and the effective magnetic moment of  $\text{CuCr}_{0.99}\text{Ln}_{0.01}\text{S}_2$  were found to decrease at temperatures below the ODT. The observed behavior of the effective magnetic moment temperature dependence in

the ODT temperature region was described as a result of copper atoms redistribution over different types of crystallographic sites.

**Supplementary Materials:** The following are available online at <https://www.mdpi.com/article/10.3390/ma14175101/s1>, Figure S1: Powder diffraction patterns of CuCrS<sub>2</sub>-matrix and CuCr<sub>0.99</sub>Ln<sub>0.01</sub>S<sub>2</sub> solid solutions, Table S1: Lattice parameters of CuCr<sub>0.99</sub>Ln<sub>0.01</sub>S<sub>2</sub>, Table S2: Elemental composition of CuCr<sub>0.99</sub>Ln<sub>0.01</sub>S<sub>2</sub>.

**Author Contributions:** Conceptualization, E.V.K. and M.M.S.; methodology, E.V.K.; investigation, E.V.K., M.M.S. and V.V.Z.; synthesis, I.Y.F.; writing—original draft preparation, E.V.K. and M.M.S.; writing—review and editing, E.V.K. and M.M.S.; visualization, E.V.K. and M.M.S.; supervision, E.V.K.; project administration, E.V.K.; funding acquisition, E.V.K. All authors have read and agreed to the published version of the manuscript.

**Funding:** This study was funded by the Russian Science Foundation (project No. 19-73-10073).

**Institutional Review Board Statement:** Not applicable.

**Informed Consent Statement:** Not applicable.

**Data Availability Statement:** The data presented in this study are available in Supplementary Materials.

**Acknowledgments:** E.V. Korotaev, M.M. Syrovkashin, and I.Yu. Filatova appreciate the Russian Science Foundation for their support. V.V. Zvereva appreciates the Ministry of Science and Higher Education of the Russian Federation (No. 121031700313-8).

**Conflicts of Interest:** The authors declare that they have no conflict of interest.

## References

- Engelsman, F.M.R.; Wieggers, G.A.; Jellinek, F.; Van Laar, B. Crystal structures and magnetic structures of some metal(I) chromium(III) sulfides and selenides. *J. Solid State Chem.* **1973**, *6*, 574–582. [\[CrossRef\]](#)
- Bongers, P.F.; Van Bruggen, C.F.; Koopstra, J.; Omlou, W.P.F.A.M.; Wieggers, G.A.; Jellinek, F. Structures and magnetic properties of some metal (I) chromium (III) sulfides and selenides. *J. Phys. Chem. Solids* **1968**, *29*, 977–984. [\[CrossRef\]](#)
- Korotaev, E.V.; Syrovkashin, M.M.; Filatova, I.Y.; Sotnikov, A.V. Effect of the Order-Disorder Transition on the Electronic Structure and Physical Properties of Layered CuCrS<sub>2</sub>. *Materials* **2021**, *14*, 2729. [\[CrossRef\]](#)
- Rasch, J.C.E.; Boehm, M.; Ritter, C.; Mutka, H.; Schefer, J.; Keller, L.; Abramova, G.M.; Cervellino, A.; Löffler, J.F. Magnetoelastic coupling in the triangular lattice antiferromagnet CuCrS<sub>2</sub>. *Appl. Phys. Lett.* **2009**, *80*, 104431.
- Karmakar, A.; Dey, K.; Chatterjee, S.; Majumdar, S.; Giri, S. Spin correlated dielectric memory and rejuvenation in multiferroic CuCrS<sub>2</sub>. *Appl. Phys. Lett.* **2014**, *104*, 052906. [\[CrossRef\]](#)
- Almukhametov, R.F.; Yakshibaev, R.A.; Gabitov, E.V.; Abdullin, A.R.; Kutusheva, R.M. Structural properties and ionic conductivities of CuCr<sub>1-x</sub>V<sub>x</sub>S<sub>2</sub> solid solutions. *Phys. Status Solidi* **2003**, *236*, 29–33. [\[CrossRef\]](#)
- Korotaev, E.V.; Syrovkashin, M.M.; Filatova, I.Y.; Pelmenev, K.G.; Zvereva, V.V.; Peregudova, N.N. Seebeck Coefficient of Cation-Substituted Disulfides CuCr<sub>1-x</sub>Fe<sub>x</sub>S<sub>2</sub> and Cu<sub>1-x</sub>Fe<sub>x</sub>CrS<sub>2</sub>. *J. Electron. Mater.* **2018**, *47*, 3392–3397. [\[CrossRef\]](#)
- Korotaev, E.V.; Syrovkashin, M.M.; Filatova, I.Y.; Trubina, S.V.; Nikolenko, A.D.; Ivlyushkin, D.V.; Zavertkin, P.S.; Sotnikov, A.V.; Kriventsov, V.V. XANES investigation of novel lanthanide-doped CuCr<sub>0.99</sub>Ln<sub>0.01</sub>S<sub>2</sub> (Ln = La, Ce) solid solutions. *Appl. Phys. A* **2020**, *126*, 537. [\[CrossRef\]](#)
- Hansen, A.-L.; Dankwort, T.; Groß, H.; Etter, M.; König, J.; Duppel, V.; Kienle, L.; Bensch, W. Structural properties of the thermoelectric material CuCrS<sub>2</sub> and of deintercalated CuxCrS<sub>2</sub> on different length scales: X-ray diffraction, pair distribution function and transmission electron microscopy studies. *J. Mater. Chem. C* **2017**, *5*, 9331–9338. [\[CrossRef\]](#)
- Al'mukhametov, R.F.; Yakshibaev, R.A.; Gabitov, E.V.; Abdullin, A.R. Investigation of superionic phase transition in the CuCr<sub>1-x</sub>V<sub>x</sub>S<sub>2</sub> system by X-ray diffraction and magnetic methods. *Phys. Solid State* **2000**, *42*, 1508–1511. [\[CrossRef\]](#)
- Tsujii, N.; Kitazawa, H.; Kido, G. Insulator to metal transition induced by substitution in the nearly two-dimensional compound CuCr<sub>1-x</sub>V<sub>x</sub>S<sub>2</sub>. *Phys. Status Solidi Curr. Top. Solid State Phys.* **2006**, *3*, 2775–2778.
- Al'mukhametov, R.F.; Yakshibaev, R.A.; Gabitov, E.V.; Abdullin, A.R. Synthesis and X-ray diffraction study of CuCr<sub>1-x</sub>V<sub>x</sub>S<sub>2</sub>. *Inorg. Mater.* **2000**, *36*, 437–440. [\[CrossRef\]](#)
- Wu, D.; Huang, S.; Feng, D.; Li, B.; Chen, Y.; Zhang, J.; He, J. Revisiting AgCrSe<sub>2</sub> as a promising thermoelectric material. *Phys. Chem. Chem. Phys.* **2016**, *18*, 23872–23878. [\[CrossRef\]](#)
- Bhattacharya, S.; Basu, R.; Bhatt, R.; Pitale, S.; Singh, A.; Aswal, D.K.; Gupta, S.K.; Navaneethan, M.; Hayakawa, Y. CuCrSe<sub>2</sub>: A high performance phonon glass and electron crystal thermoelectric material. *J. Mater. Chem. A* **2013**, *1*, 11289–11294. [\[CrossRef\]](#)
- Guy, D.R.P.; Marseglia, E.A.; Guy, S.C. Electron Spin Resonance in CuCrS<sub>2</sub> and CuCrSe<sub>2</sub> Single Crystals. *Mol. Cryst. Liq. Cryst.* **1985**, *121*, 165–168. [\[CrossRef\]](#)

16. Akmanova, G.R.; Davletshina, A.D. Ionic conductivity and diffusion in superionic conductors  $\text{CuCrS}_2\text{-AgCrS}_2$ . *Lett. Mater.* **2013**, *3*, 76–78. [[CrossRef](#)]
17. Abramova, G.M.; Petrakovskii, G.A. Metal-insulator transition, magnetoresistance, and magnetic properties of 3d-sulfides (Review). *Low Temp. Phys.* **2006**, *32*, 725–734. [[CrossRef](#)]
18. Tsujii, N.; Kitazawa, H. Substitution effect on the two-dimensional triangular-lattice system  $\text{CuCrS}_2$ . *J. Phys. Condens. Matter* **2007**, *19*, 145245. [[CrossRef](#)]
19. Al'mukhametov, R.F.; Yakshibaev, R.A.; Gabitov, É.V. Magnetic and transport properties of  $\text{CuCr}_{1-x}\text{V}_x\text{S}_2$  compounds. *Phys. Solid State* **1999**, *41*, 1327–1328. [[CrossRef](#)]
20. Vasilyeva, I.G. Chemical aspect of the structural disorder in  $\text{CuCrS}_2$  and  $\text{CuCr}_{1-x}\text{V}_x\text{S}_2$  solid solutions. *J. Struct. Chem.* **2017**, *58*, 1009–1017. [[CrossRef](#)]
21. Korotaev, E.V.; Syrokvashin, M.M.; Filatova, I.Y.; Zvereva, V.V. Vanadium doped layered copper-chromium sulfides: The correlation between the magnetic properties and XES data. *Vacuum* **2020**, *179*, 109390. [[CrossRef](#)]
22. Zhang, J.Y.; Zhu, J.H.; You, L.; Guo, K.; Li, Z.L.; Lin, W.G.; Huang, J.; Luo, J. Enhanced and stabilized n-type thermoelectric performance in  $\alpha\text{-CuAgSe}$  by Ni doping. *Mater. Today Phys.* **2019**, *10*, 100095. [[CrossRef](#)]
23. Tewari, G.C.; Tripathi, T.S.; Rastogi, A.K. Thermoelectric properties of layer-antiferromagnet  $\text{CuCrS}_2$ . *J. Electron. Mater.* **2010**, *39*, 1133–1139. [[CrossRef](#)]
24. Abramova, G.M.; Petrakovskii, G.A.; Vorotynev, A.M.; Velikanov, D.A.; Kiselev, N.I.; Bovina, A.F.; Szymczak, R.; Al'mukhametov, R.F. Phase transitions and colossal magnetoresistance in  $\text{CuV}_x\text{Cr}_{1-x}\text{S}_2$  layered disulfides. *JETP Lett.* **2006**, *83*, 118–121. [[CrossRef](#)]
25. Inorganic Crystal Structure Database, Version 2.1.0. Leibniz Institute for Information Infrastructure, FIZ Karlsruhe, Eggenstein-Leopoldshafen, Germany, (n.d.). Available online: <https://icsd.products.fiz-karlsruhe.de/> (accessed on 17 August 2021).
26. Vassilieva, I.G.; Kardash, T.Y.; Malakhov, V.V. Phase transformations of  $\text{CuCrS}_2$ : Structural and chemical study. *J. Struct. Chem.* **2009**, *50*, 288–295. [[CrossRef](#)]
27. Selwood, P. *Magnetochemistry*, 2nd ed.; Interscience Publishers: New York, NY, USA, 1956.
28. Le Nagard, N.; Collin, G.; Gorochov, O. Etude structurale et proprietes physiques de  $\text{CuCrS}_2$ . *Mater. Res. Bull.* **1979**, *14*, 1411–1417. [[CrossRef](#)]
29. Moeller, T. *The Chemistry of the Lanthanides*; Elsevier: Amsterdam, The Netherlands, 1973.
30. Korotaev, E.V.; Syrokvashin, M.M.; Filatova, I.Y.; Trubina, S.V.; Nikolenko, A.D.; Ivlyushkin, D.V.; Zavertkin, P.S.; Kriventsov, V.V. The conduction band of the lanthanide doped chromium disulfides  $\text{CuCr}_{0.99}\text{Ln}_{0.01}\text{S}_2$  ( $\text{Ln}=\text{La}, \text{Ce}, \text{Gd}$ ): XANES investigations. In Proceedings of the AIP Conference, Novosibirsk, Russian, 13–16 July 2020; Volume 2299, p. 080004.
31. Adachi, H.; Ino, H. A ferromagnet having no net magnetic moment. *Nature* **1999**, *401*, 148–150. [[CrossRef](#)]
32. Murphy, D.W.; Chen, H.S.; Tell, B. Superionic Conduction in  $\text{AgCrS}_2$  and  $\text{AgCrSe}_2$ . *J. Electrochem. Soc.* **1977**, *124*, 1268–1271. [[CrossRef](#)]
33. Korotaev, E.V.; Syrokvashin, M.M.; Peregudova, N.N.; Kanazhevskii, V.V.; Mazalov, L.N.; Sokolov, V.V. Effects of the nearest-neighbor environment of copper atoms on the XANES spectra of layered chromium-copper disulfides. *J. Struct. Chem.* **2015**, *56*, 596–600. [[CrossRef](#)]
34. Korotaev, E.V.; Kanazhevskiy, V.V.; Peregudova, N.N.; Syrokvashin, M.M.; Mazalov, L.N.; Sokolov, V.V.; Filatova, I.Y.; Pichugin, A.Y. Xanes of X-ray absorption K edges of chromium dichalcogenides  $\text{CuCr}_{1-x}\text{M}'_x\text{S}_2$  and  $\text{MCrX}_2$ . *J. Struct. Chem.* **2016**, *57*, 1355–1361. [[CrossRef](#)]